

# Dynamic Viscoelastic Properties of Carbon Black Loaded Closed-Cell Microcellular Ethylene–Propylene–Diene Rubber Vulcanizates: Effect of Blowing Agent, Temperature Frequency, and Strain

K. C. GURIYA and D. K. TRIPATHY\*

Rubber Technology Centre, Indian Institute of Technology, Kharagpur, India

## SYNOPSIS

Dynamic mechanical analysis of carbon black loaded solid and closed-cell microcellular ethylene–propylene–diene (EPDM) vulcanizates was studied at four frequencies of 3.5, 11, 35, and 110 Hz and temperatures from  $-100$  to  $150^{\circ}\text{C}$ . A plot of the log of the storage modulus bears a linear relationship with the log of density for solid as well as closed-cell microcellular rubber. The slope of the line is found to be temperature-dependent. The relative storage modulus decreases with decrease in the relative density. It was also observed that the storage modulus and  $\tan \delta$  are both frequency- and temperature-dependent. The storage modulus results are superposed to form master curves of the modulus vs. log temperature-reduced frequency, using shift factors calculated by the Arrhenius equation. Strain-dependent isothermal dynamic mechanical analysis was carried out for DSA varying from 0.07 to 5%. The effect of blowing agent loading on the storage modulus ( $E'$ ) and loss tangent ( $\tan \delta$ ) were also studied. Cole–Cole plots of microcellular rubber shows a circular arc relationship with the density. Plots of  $\tan \delta$  against  $E'$  were found to exhibit a linear relationship. © 1996 John Wiley & Sons, Inc.

## INTRODUCTION

The dynamic mechanical response of vulcanized closed-cell microcellular rubber is an important criteria of evaluation for its use in various engineering applications. Microcellular ethylene–propylene–diene (EPDM) rubber is widely used in packaging and sealing applications due to its excellent weathering and aging properties. Although studies on the physical properties of flexible microcellular and cellular elastomers as well as thermoplastics have been reported in the literature, very little work on dynamic mechanical spectra of cellular and microcellular rubber have been reported. Previous workers<sup>1,2</sup> reported that the log shear modulus bears a linear relationship with log density for various polyurethane foams and showed

that the values of shear modulus (SM) follow the equation  $SM = a\rho^b$ , where  $a$  and  $b$  are constant and  $\rho$  is the density. Turner and co-workers<sup>3</sup> studied the dynamic mechanical response of flexible polyurethane foam specimens as well as of a compression-molded plaque of the same material to characterize the morphological structure in the foam. A theoretical treatment of pneumatic damping of open-cell foam was given by Kosten and Zwikker.<sup>4</sup> The studies on the resistance of air flow and permeability in the open-cell foam was undertaken by Gent and Rusch.<sup>5</sup> Gent and Rusch also described a model for the viscoelastic behavior of open-cell foams.<sup>6</sup> Ringe and Hoge<sup>7,8</sup> reported the construction of the master curve of the dynamic shear modulus of polystyrene bead foams and solid polymer for a range of frequencies as well as for a wide range of temperature. Jackson and co-workers<sup>9</sup> reported the linear elastic properties of microcellular plastics. Strain-dependent dynamic properties of microcellular rubber are also of limited study in the

\* To whom correspondence should be addressed.

literature. However, several workers<sup>10-19</sup> reported strain-dependent dynamic mechanical properties of solid rubbers.

The objective of the present work was to investigate the viscoelastic properties of carbon black-filled EPDM-based microcellular rubber. The effect of the blowing agent (density), temperature, and frequency on the dynamic mechanical properties of closed-cell microcellular rubber was studied. In addition, the strain-dependent isothermal dynamic mechanical properties of microcellular rubber were also investigated.

## EXPERIMENTAL

### Materials

The rubber used was EPDM rubber [Kelton 520], of ethylene content 55 mol %, diene content 4.5 mol % (DCPD), and specific gravity 0.86, manufactured by DSM Chemicals, Holland. The carbon black (HAF-N330) used as a filler was manufactured by Philips Carbon Black Ltd., India. Its characteristics were as follows: specific gravity, 1.81, and particle size, 26–30 nm. The dicumyl peroxide (DCP) used was Percidol 540C (40% DCP on an inert filler), manufactured by Chemoplast(I) Ltd. DNPT was used as a blowing agent, manufactured by High Polymer Labs, India.

### Compounding and Sample Preparation

The rubber was compounded with other ingredients according to the formulations of the mixes (Table I) and the blowing agent was added at the end. For obtaining cure characteristics of the compounds, a Monsanto rheometer (R-100) was used. The compounds were molded at 160°C to 80% of their respective cure times. All sides of the mold were tapered to 30° to facilitate the expansion of the molded compounds to closed-cell, nonintercommunicating microcellular products with a better mold release. Expanded microcellular sheets were postcured at 100°C for 1 h in an electrically heated air oven.

### Dynamic Mechanical Analysis

Dynamic mechanical analysis of both filled and unfilled microcellular EPDM rubber was determined as a function of temperature and strain with the help of the Rheovibron DDV III EP of Orientec Corp., Japan. Test pieces were in strip form with approximate dimensions of 0.6 × 0.3 × 0.5 cm. Tests

**Table I** Formulation of the Mixes

	Mix No.			
	EB <sub>20</sub>	EB <sub>22</sub>	EB <sub>24</sub>	EB <sub>26</sub>
EPDM	100	100	100	100
ZnO	2	2	2	2
Stearic acid	2	2	2	2
HAF	30	30	30	30
Paraffin oil	9	9	9	9
DCP (40%)	2	2	2	2
DNPT	0	2	4	6

were carried out at four frequencies (3.5, 11, 35, and 110 Hz) over a temperature range of -100 to 150°C with a dynamic strain of 0.18%. For the measurement of strain-dependent dynamic mechanical properties, all tests were carried out at 27 ± 2°C and at a frequency of 11 Hz. The test piece length was varied so as to cover a range of double-strain amplitude (DSA) from 0.07 to 5%. DSA =  $\Delta L/L_0$ , where  $\Delta L$  = strain and  $L_0$  = length of the test piece.

## RESULTS AND DISCUSSION

### Temperature-dependent Dynamic Mechanical Properties

#### Effect of Blowing Agent

Figure 1 describes the variation of storage modulus,  $E'$ , at 11 Hz with temperature for 30 phr carbon black-filled closed-cell microcellular EPDM rubber vulcanizates with different loadings of the blowing agent. The nature of storage modulus vs. temperature plots of the closed-cell microcellular rubber is similar to that of the solid rubber. In the glassy region, the storage modulus  $E'$  is found to decrease with increase in blowing agent loadings. The deformation of the enclosed gas in the closed cell is elastic in nature and has little effect on the storage modulus. Hence, the storage modulus decreases concomitantly with decrease in the solid rubber contents vis-à-vis density.<sup>8</sup>

The storage modulus of the solid and microcellular rubber are plotted against density at three temperatures (-100, 50, and 100°C) in Figure 2. From the logarithmic plot, a linear relationship is evident which obeys the following relation: storage modulus (SM) =  $a \times [\text{density } (d)]^b$ , where  $a$  and  $b$  are constants at a particular temperature and vary with the change of temperature. In the plot,  $b$  denotes the slope of the line, the values of which at

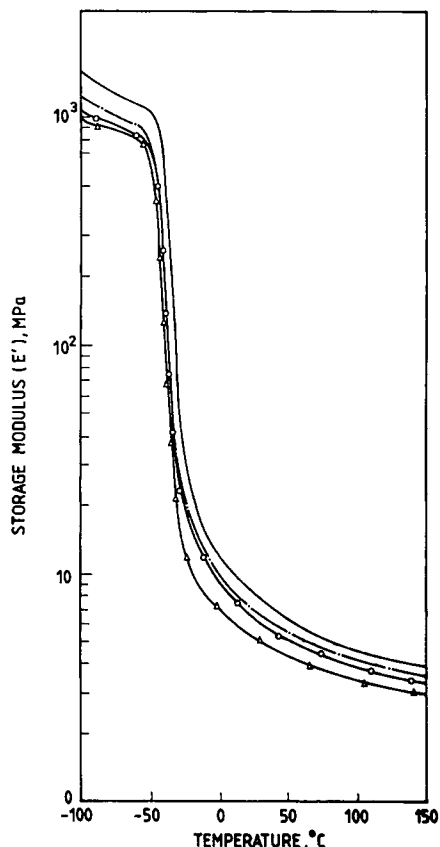


**Figure 1** Plots of storage modulus ( $E'$ ) vs. temperature of 30 phr carbon black filled EPDM vulcanizates—effect of blowing agent loading: (—) EB<sub>20</sub>; (—●—) EB<sub>22</sub>; (—○—) EB<sub>24</sub>; (—△—) EB<sub>26</sub>.

−100, 50, and 100°C are 1.66, 1.39, and 1.06, respectively. It is evident from the data that the slope decreases with increase in temperature. It means that the rate of increase of the storage modulus with density at higher temperature is less compared to the same at lower temperature. This is because at lower density a greater number of cells are formed which increase the gas pressure at higher temperature, leading to enhancement of the storage modulus. Thus, at higher temperature, the relative decrease in the storage modulus is less with a decrease in density as compared to the lower temperature.

The plots of relative storage modulus ( $E'_f/E'_s$ ) of 30 phr carbon black-loaded solid and microcellular compounds at three temperatures (−100, 50, and 100°C) are shown in Figure 3. With decrease in the relative density, the relative storage modulus decreases at all temperatures. From the figure it is also evident that at any relative density the relative storage modulus of closed-cell microcellular rubber shows a higher value with increase in temperature (−100, 50, 100°C).

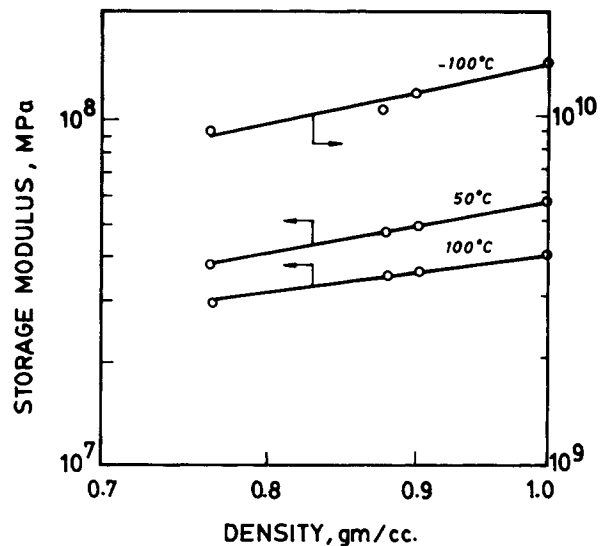


**Figure 2** Plots of storage modulus ( $E'$ ) vs. density of 30 phr carbon black filled EPDM vulcanizates at different temperatures.

The variation of the loss tangent ( $\tan \delta$ ) with temperature for the 30 phr carbon black filled solid as well as closed-cell microcellular rubber vulcanizates are shown in Figure 4. These figures exhibit the damping behavior of the closed-cell microcellular rubber vulcanizates with variation of the blowing agent loading.  $\tan \delta$  values corresponding to the glass transition temperature are shown in Table II. In the rubbery region ( $>40^\circ\text{C}$ ), the  $\tan \delta$  value decreases with increase in blowing agent loading up

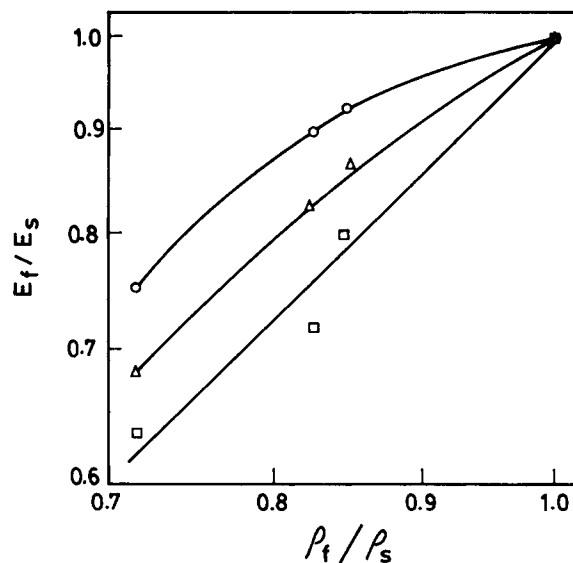


**Figure 3** Plots of relative storage modulus ( $E'_f/E'_s$ ) vs. relative density ( $\rho_f/\rho_s$ ); (—●—) −100°C; (—△—) 50°C; (—○—) 100°C.

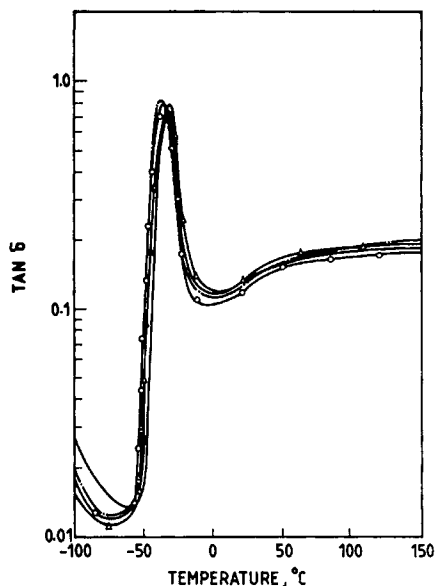


**Figure 4** Plots of loss tangent ( $\tan \delta$ ) vs. temperature of 30 phr carbon black filled EPDM vulcanizates—effect of blowing agent loading: (—) EB<sub>20</sub>; (—●—) EB<sub>22</sub>; (—○—) EB<sub>24</sub>; (—△—) EB<sub>26</sub>.

to 4 phr. Again, at 6 phr, the blowing agent loading  $\tan \delta$  value increases as compared to 2 and 4 phr blowing agent loading. The enclosed gas in the closed cell has little contribution toward the damping property. But in case of the open cell, the damping behavior is largely affected by the viscosity of the fluid.<sup>6</sup> For closed-cell microcellular rubber for a higher blowing agent loading, the decomposed gas pressure in the closed cell increases.<sup>22</sup> This causes stress on the cell membrane and the cell membrane remains in a strained condition. This increase in strain to some extent increases the  $\tan \delta$  value, i.e., damping. This has also been observed in the case of strain-dependent dynamic mechanical properties.

**Effect of Frequency**

The storage modulus ( $E'$ ) of carbon black loaded microcellular rubber vulcanizates at four frequencies ( $f$ ) of 3.5, 11, 35, and 110 Hz and at temperature

**Table II Glass Transition Temperature ( $T_g$ ) Carbon Black Filled Microcellular Rubber**

	Mix No.			
	EB <sub>20</sub>	EB <sub>22</sub>	EB <sub>24</sub>	EB <sub>26</sub>
$T_g$ (°C)	-30.7	-34.6	-33.1	-32.6
Tan $\delta$	0.86	0.92	0.88	0.91

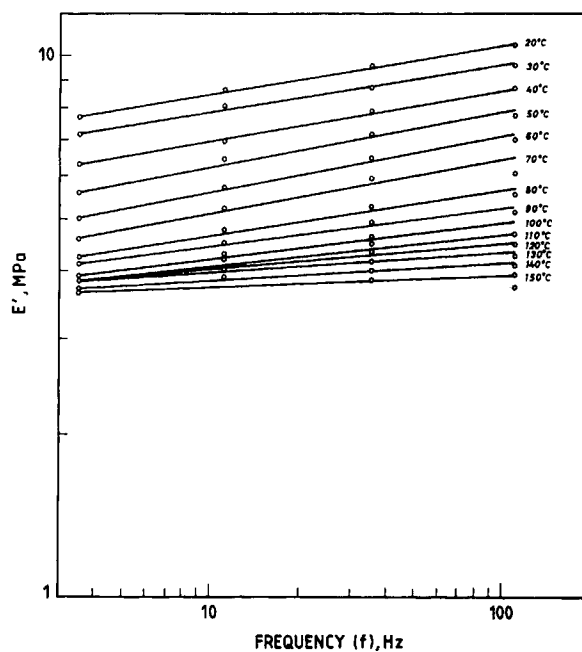


**Figure 5** Plots of storage modulus ( $E'$ ) vs. frequency ( $f$ ) at temperature ( $>T_g$ ) of carbon black filled solid EPDM vulcanizates.

varying from 20 to 150°C are plotted in Figures 5–8. All data were taken on a single specimen. These data were obtained to define the time–temperature dependence of the modulus of microcellular rubber. A logarithmic plot of  $E'$  vs.  $f$  shows that the storage

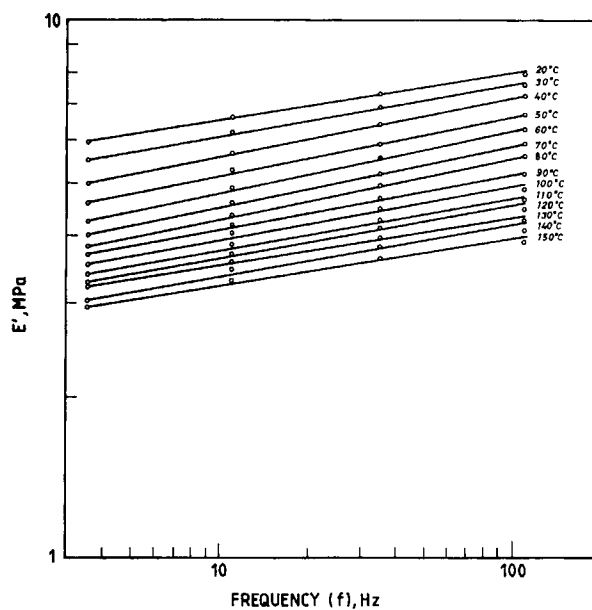


**Figure 6** Plots of storage modulus ( $E'$ ) vs. frequency ( $f$ ) at temperature ( $>T_g$ ) of carbon black filled 2 phr blowing agent-loaded EPDM vulcanizates.

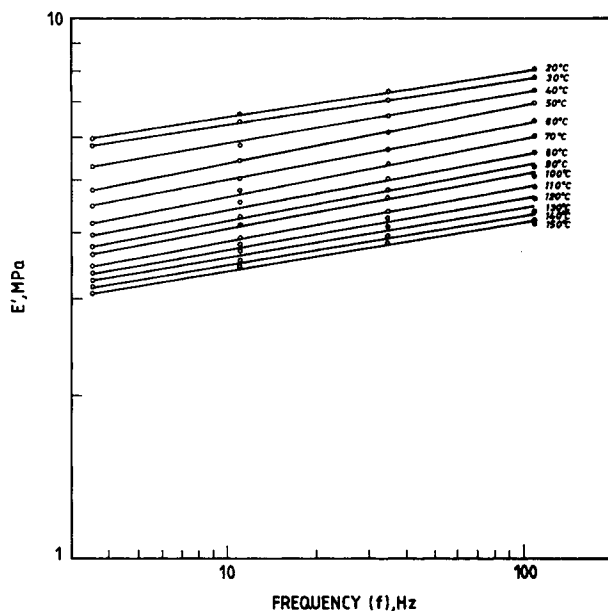


**Figure 7** Plots of storage modulus ( $E'$ ) vs. frequency ( $f$ ) at temperature ( $>T_g$ ) of carbon black filled 4 phr blowing agent-loaded EPDM vulcanizates.

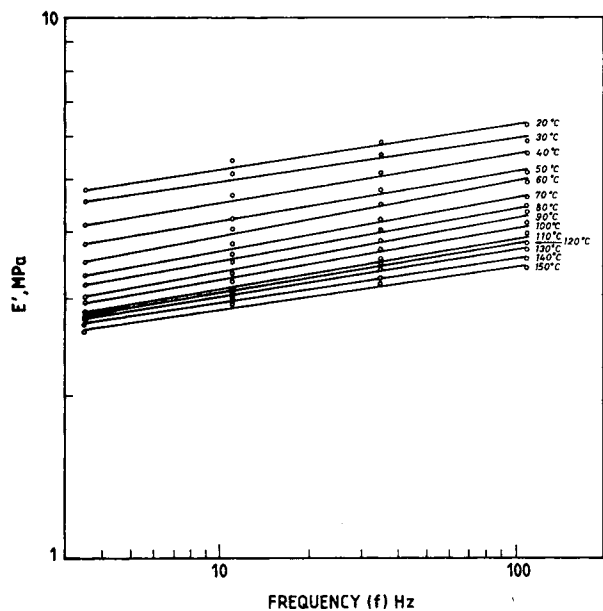


**Figure 8** Plots of storage modulus ( $E'$ ) vs. frequency ( $f$ ) at temperature ( $>T_g$ ) of carbon black filled 6 phr blowing agent-loaded EPDM vulcanizates.

modulus is strain rate-dependent with the modulus increasing with frequency at all temperatures. Also, the rate dependence decreases at high temperature. These curves are shifted along the  $f$  axis to obtain superposition. The resulting shift factors ( $\log a_T$ ) at any temperature for the storage modulus is obtained with respect to room temperature (30°C). The  $\log a_T$  values are plotted against  $10^3/T$  in Figure 9 to calculate the activation energy ( $\Delta H$ ) value by the Arrhenius equation

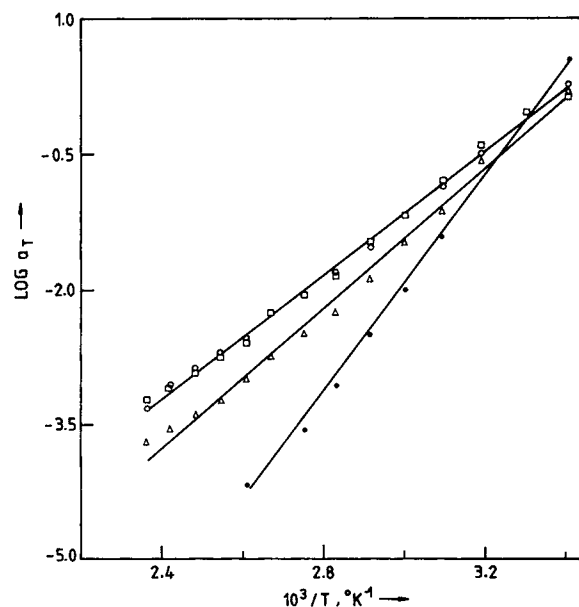
$$\log a_T = \frac{\Delta H}{2.303R} \left( \frac{1}{T} - \frac{1}{T_0} \right)$$

where  $T_0 = 303$  K,  $\log a_T$  is the shift factor,  $\Delta H$  is the activation energy, and  $R$  is the gas constant. From the straight-line plot of Figure 9, the slope of the line, i.e.,  $\Delta H$  values, is calculated for both solid and microcellular rubber.  $\Delta H$  values for the solid was found to be 28 kcal/mol, where the same for the microcellular rubber is almost equal to 16 kcal/mol.

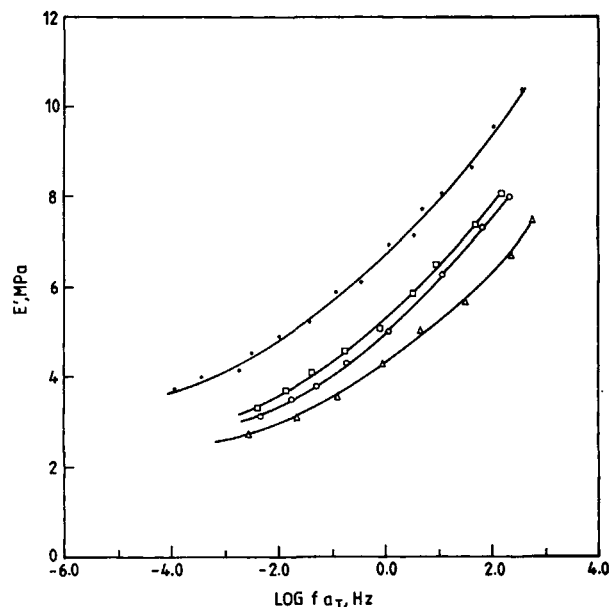
The data from Figures 5–8 are replotted in Figure 10 as  $E'$  vs.  $\log fa_T$  using  $a_T$  from the Arrhenius equation,  $f$  being the frequency in cycles/s to obtain the master curves of  $\log E'$  vs.  $\log fa_T$  corresponding to the three microcellular EPDM rubber and the solid polymer. The curves represent the storage modulus of these materials at 30°C.

Figure 11 shows the plots of loss tangent with temperature for 2 phr blowing agent-loaded micro-

cellular rubber at four frequencies of 3.5, 11, 35, and 110 Hz. The loss tangent value decreases with decrease of frequency at a temperature below the glass transition temperature ( $T_g$ ). The  $T_g$  decreases and shifts toward high temperature with increased frequency. However, beyond  $T_g$ , up to 50°C, the  $\tan \delta$  value decreases with the increase in frequency. With



**Figure 9**  $\log a_T$  vs. temperature plots: (●) EB<sub>20</sub>; (□) EB<sub>22</sub>; (○) EB<sub>24</sub>; (△) EB<sub>26</sub>.



**Figure 10** Master curves of the storage modulus of solid and microcellular rubber vulcanizates: (●) EB<sub>20</sub>; (□) EB<sub>22</sub>; (○) EB<sub>24</sub>; (△) EB<sub>26</sub>.

further increase in temperature, the trend is reversed. This phenomenon may be explained by the “pseudorigidity” effect of the frequency.<sup>20</sup> In this effect, the relaxation time responsible for chain mobility reduces drastically with increasing frequency, which results in temporary freezing of the amorphous chain. At high temperature, this effect is minimized and the trend is reversed. Other blowing agent loadings show similar results.

### Strain-dependent Dynamic Mechanical Properties

#### Storage Modulus

At the lowest imposed strain amplitude, both solid and closed-cell microcellular rubber vulcanizates show the highest storage modulus ( $E'$ ). At the lowest DSA (0.07%), the three-dimensional filler-polymer, filler-filler, and entrapped decomposed gas (closed-cell) structure acts as a rigid unit against the imposed strain and, hence, it shows the highest modulus value. The low strain is not capable of causing any significant change in the network structure. Figure 12 shows that the absolute modulus value decreases with increases in blowing agent loading in 30 phr carbon black loaded closed-cell microcellular compounds at room temperature. The figure also shows the insensitivity to the strain effect below 1% DSA. As blowing agent loading increases, the thickness of the cell membrane reduces and the stiffness of the

compounds decreases, which results in lower storage modulus. The fall of storage modulus above 1% DSA is sharp with increasing strain. This may be due to the collapse of a weak cell membrane with increase in strain amplitude.

#### Loss Tangent

$\tan \delta$  vs. DSA plots of solid and microcellular vulcanizates of a 30 phr carbon black-loaded compound with variation of the blowing agent are shown in Figure 13. The loss tangent increases slowly with increases in strain. In the closed-cell microcellular rubber, the bending, buckling, and extension of the cell membrane<sup>21,22</sup> occurs at low strain and, hence, the  $\tan \delta$  value shows a higher value than does the solid vulcanizates. In high-strain regions, i.e., above 1% DSA, the loss tangent value increases sharply due to the breakdown of the filler aggregates in the solid vulcanizates, whereas in the case of microcellular rubber, another factor, i.e., jamming and collapse of the cell membrane, also plays an important role in increasing the loss tangent value.

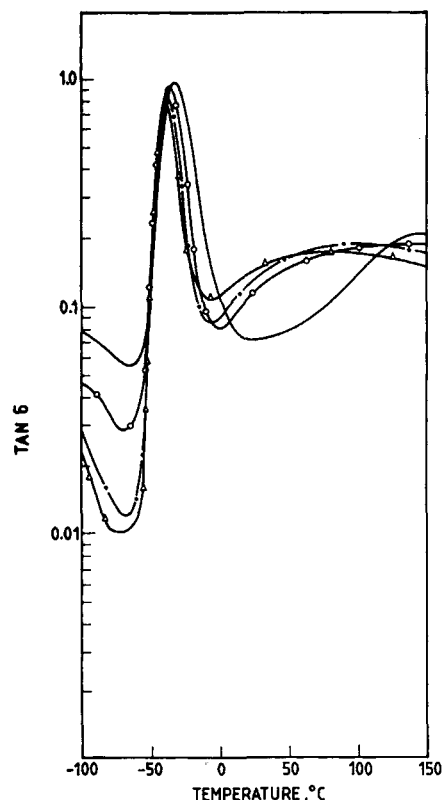


**Figure 11** Plots of loss tangent ( $\tan \delta$ ) vs. temperature of 30 phr carbon black filled EPDM vulcanizates—effect of frequency: (—) 110 Hz; (—○—) 35 Hz; (—●—) 11 Hz; (—△—) 3.5 Hz.

### $E'$ and $E''$ Relationship

The relationships between  $E'$  and  $E''$  for 30 phr carbon black loaded closed-cell microcellular EPDM vulcanizates over a wide range of DSA from 0.07 to 5% are illustrated in Figure 14. These Cole-Cole plots<sup>14,23,24</sup> of the complex dynamic modulus represent the amplitude dependence of its components  $E'$  and  $E''$ . It is evident from the figure that the circular arc relationship holds good for the closed-cell microcellular rubber vulcanizates. Each point along the arc corresponds to a different amplitude of vibration. It is seen that the circular arc decreases with increase in the blowing agent loading. At lower amplitude, the storage modulus shows a higher value as a result of the elastic buckling or extension of the cell walls of closed-cell microcellular rubber. Due to the breakdown of some cell walls at higher amplitude, both storage and loss modulus decrease, which corresponds to the circular arc relationship.<sup>21</sup>

### $\tan \delta$ and $E'$ Relationship

Interrelationships between the dynamic parameters act as a guideline for understanding their origin. Medalia and Laube reported the following simple relation for  $\tan \delta$  with the modulus for natural rubber at 10% DSA and at 25°C<sup>25</sup>:

$$\tan \delta = 0.033 + 0.0449(E_{1\%} - E_{10\%})^{1/2}$$

Even though mathematically defined for model system, the dynamic mechanical properties of polymeric

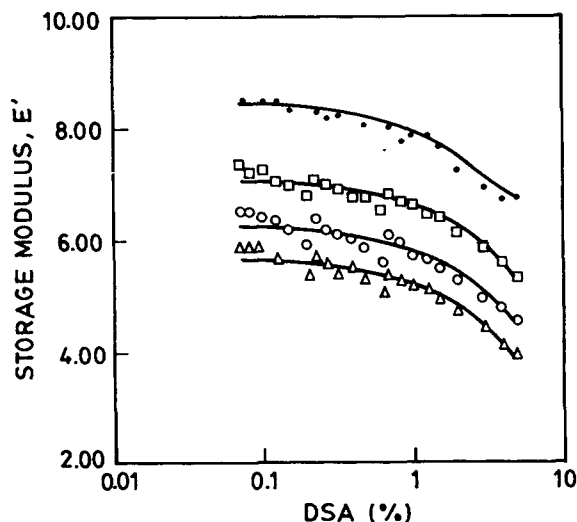


**Figure 12** Storage modulus ( $E'$ ) as a function of DSA of 30 phr carbon black filled EPDM vulcanizates—effect of blowing agent loading: (●) EB<sub>20</sub>; (□) EB<sub>22</sub>; (○) EB<sub>24</sub>; (△) EB<sub>26</sub>.

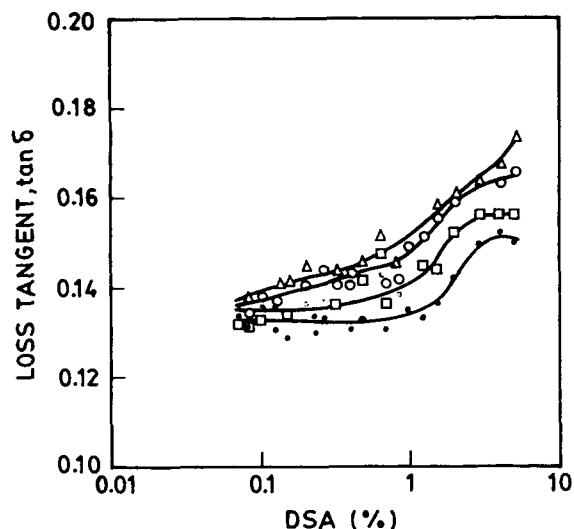


**Figure 13** Loss tangent ( $\tan \delta$ ) as a function of DSA of 30 phr carbon black filled EPDM vulcanizates—effect of blowing agent: (●) EB<sub>20</sub>; (□) EB<sub>22</sub>; (○) EB<sub>24</sub>; (△) EB<sub>26</sub>.

system may show different types of dependence on one another, especially when fillers are incorporated. A linear relationship between  $\tan \delta$  and  $\log E'$  was also established by Namboodiri et al.<sup>17</sup> for black-filled EPDM vulcanizates. Figure 15 shows the plot of  $\tan \delta$  as a function of  $\log E'$  for 30 phr carbon black loaded closed-cell microcellular EPDM vulcanizates with varying blowing agent loading (density). The linear nature of the plot could be mathematically expressed as  $\tan \delta = m \log E' + C_1$ , where  $m$  is the slope of line and  $C_1$  is a constant. With incorporation of the blowing agent, the slope ( $m$ ) changes compared to the solid rubber vulcanizates, but with variation of the blowing agent loading, the slope remains almost unchanged. The existence of such a relation when a purely hysteric parameter is related to a purely elastic parameter shows that the primary cause is the same origin, most probably the filler–filler interaction and deformation of entrapped air in the closed cell.

### CONCLUSION

The following conclusions have been drawn from the above studies:

1. The storage modulus ( $E'$ ) or stiffness of the microcellular rubber decreases concomitantly with increasing blowing agent loading. A log-log plot of the storage modulus shows a linear relationship with density at all temperatures. With increase in temperature, the slope of

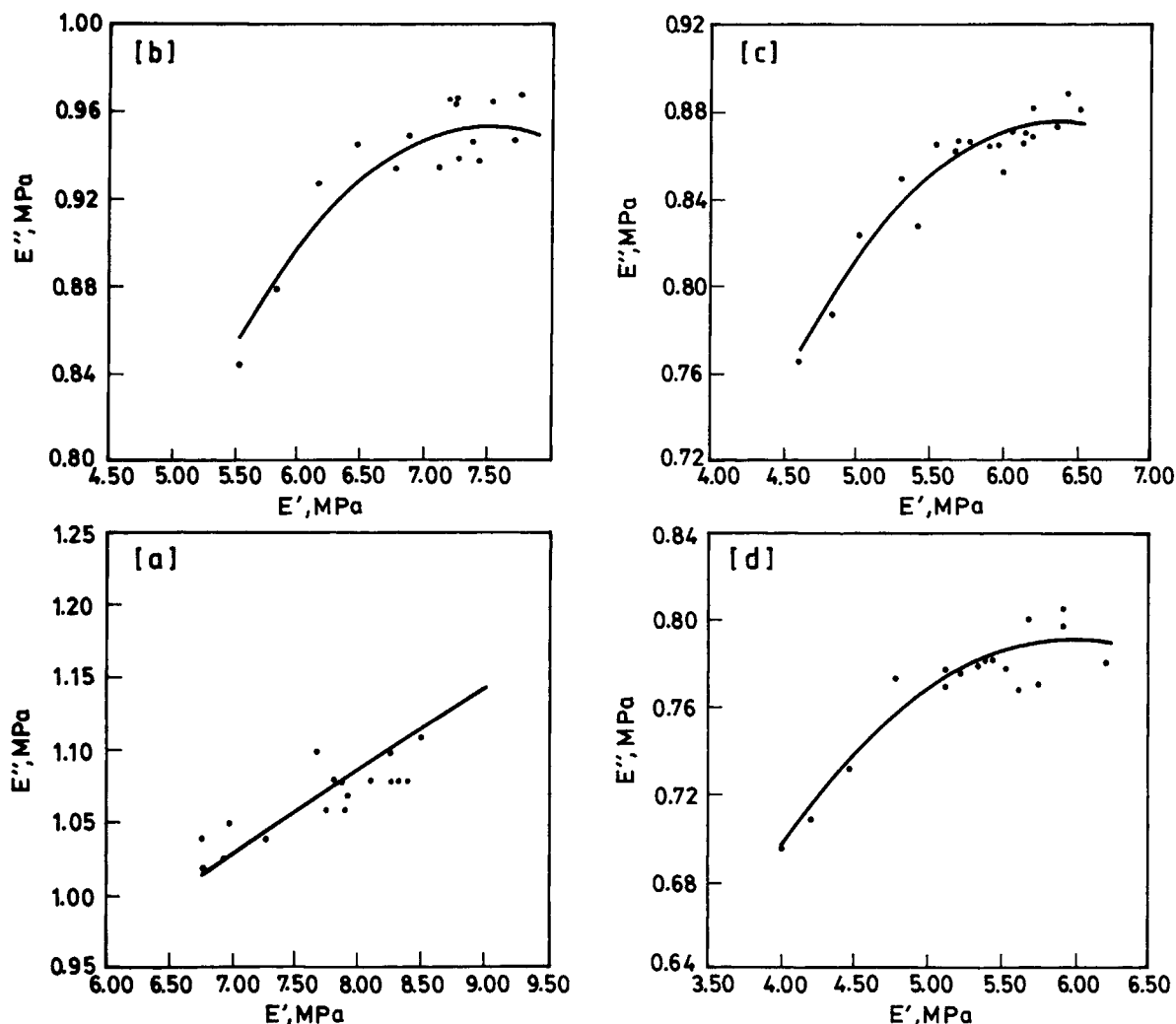


Figure 14  $E'$  and  $E''$  relationships of 30 phr carbon black filled EPDM vulcanizates—effect of blowing agent. (a)  $EB_{20}$ ; (b)  $EB_{22}$ ; (c)  $EB_{24}$ ; (d)  $EB_{26}$ .

the straight line decreases, i.e., the rate of the decrease of the storage modulus with density increases.

2. The relative storage modulus ( $E_f/E_s$ ) decreases with decrease in relative density ( $\rho_f/\rho_s$ ). At any relative density, the relative storage modulus shows a higher value with increasing temperature.
3. In the rubbery region, damping ( $\tan \delta$ ) properties of the carbon black-loaded microcellular rubber exhibits almost constant values over a wide range of temperature.
4. The storage modulus is found to be frequency (i.e., strain rate)-dependent. With increase in frequency, the storage modulus increases at all temperatures. Master curves of modulus vs. log-reduced strain rate are formed by a time-temperature superposition method, us-

ing shift factors calculated from the Arrhenius equation for solid and microcellular rubber.

5. The frequency-dependent loss tangent plot of 2 phr blowing agent-loaded closed-cell microcellular rubber shows that around  $50^\circ\text{C}$  the  $\tan \delta$  value decreases due to temporary freezing of chains occurring at high frequency.
6. The storage modulus of 30 phr carbon black loaded microcellular vulcanizates decreases with increase in blowing agent loading at low strain. At higher strain, i.e., beyond 1% DSA, the storage modulus drops sharply for all microcellular rubber. However, the loss tangent shows a reverse trend.
7. The plots of  $E'$  vs.  $E''$  for 30 phr carbon black filled microcellular rubber vulcanizates ex-



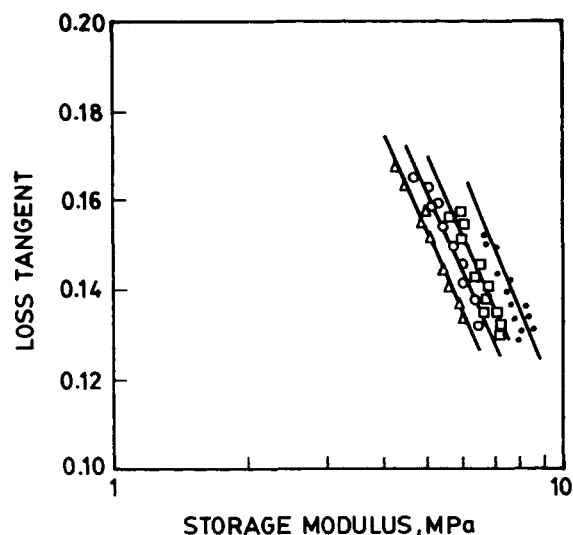


**Figure 15**  $\tan \delta$  and  $E'$  plots of microcellular EPDM vulcanizates: (●) EB<sub>20</sub>; (□) EB<sub>22</sub>; (○) EB<sub>24</sub>; (△) EB<sub>26</sub>.

hibit a circular arc relationship. It is seen that the circular arc decreases with increase in blowing agent loading.

8. Empirical relationships between  $\tan \delta$  and  $E'$  for microcellular rubber have been found to be linear, the slope of which is independent of blowing agent loading.

This work is supported by a research grant from the Council of Scientific and Industrial Research, Government of India.

## REFERENCES

1. F. M. Kujawa, *J. Cell Plast.*, **1**, 400 (1965).
2. H. Briscoll and C. R. Thomas, *Br. Plast.*, **79**, July 1968.
3. R. B. Turner, H. L. Spell, and G. L. Wilkes, *Proc. SPI 28th Ann. Tech. Market Conf.*, 224 (1984).
4. C. W. Kosten and C. Zwikker, *Rubb. Chem. Technol.*, **12**, 105 (1939).
5. A. N. Gent and K. C. Rusch, *J. Cell. Plast.*, **2**, 46 (1966).
6. A. N. Gent and K. C. Rusch, *Rubb. Chem. Technol.*, **39**, 389 (1966).
7. J. A. Rinde and K. G. Hoge, *J. Appl. Polym. Sci.*, **15**, 1377 (1971).
8. J. A. Rinde and K. G. Hoge, *J. Appl. Polym. Sci.*, **16**, 1409 (1972).
9. C. L. Jackson, M. T. Show, and J. H. Auburt, *Polymer*, **32**(2), 221 (1991).
10. A. R. Payne, *J. Appl. Polym. Sci.*, **8**, 266 (1964).
11. A. R. Payne, *J. Appl. Polym. Sci.*, **7**, 873 (1963).
12. A. R. Payne, *Rubb. Chem. Technol.*, **37**(5), 1190 (1964).
13. A. K. Sircar and T. G. Lamond, *Rubb. Chem. Technol.*, **48**, 79 (1975).
14. N. K. Dutta and D. K. Tripathy, *Kautsch. Gummi. Kunstst.*, **42**, 665 (1989).
15. L. F. Byrne and D. J. Hourston, *J. Appl. Polym. Sci.*, **23**, 1607 (1979).
16. L. F. Byrne and D. J. Hourston, *J. Appl. Polym. Sci.*, **23**, 2899 (1979).
17. C. S. S. Namboodiri, D. K. Tripathy, and P. L. Salinkar, *Kautsch. Gummi. Kunstst.*, **43**, 770 (1990).
18. D. R. Hazlton and R. C. Puydak, *Rubb. Chem. Technol.*, **44**, 1043 (1971).
19. C. S. S. Namboodiri and D. K. Tripathy, *Plast. Rubb. Comp. Process. Appl.*, **17**, 171 (1992).
20. R. F. Boyer, *J. Polym. Sci. Part C.*, **14**, 267 (1966).
21. K. C. Guriya and D. K. Tripathy, *J. Elast. Plast.*, **27**(4), 305 (1995).
22. L. J. Gibson and M. F. Ashby, *Cellular Solids, Structure and Properties*, Pergamon Press, Oxford, 1988.
23. K. Mukhopadhyay, D. K. Tripathy, and S. K. De, *J. Appl. Polym. Sci.*, **48**, 1089 (1993).
24. K. Mukhopadhyay and D. K. Tripathy, *J. Elast. Plast.*, **24**, 203 (1993).
25. A. Medalia and S. G. Laube, *Rubb. Chem. Technol.*, **51**, 89 (1978).

Received October 6, 1995

Accepted February 13, 1996